



Published in final edited form as:

Mol Imaging Biol. 2009 ; 11(5): 303–307. doi:10.1007/s11307-009-0209-0.

Replacing ^{99m}Tc with ^{111}In improves MORF/cMORF pretargeting by reducing intestinal accumulation

Guozheng Liu, Dengfeng Cheng, Shuping Dou, Xiangji Chen, Minmin Liang, P Hendrik Pretorius, Mary Ruszkowski, and Donald J Hnatowich

Division of Nuclear Medicine, Department of Radiology, University of Massachusetts Medical School, 55 Lake Ave North, Worcester, MA 01655

Abstract

Purpose—To reduce accumulation in the abdomen by MORF/cMORF pretargeting, ^{111}In was compared to ^{99m}Tc as the radiolabel.

Procedures—After receiving either ^{99m}Tc (MAG3)-cMORF or ^{111}In (DTPA)-cMORF, normal mice were imaged and sacrificed for pharmacokinetics. Thereafter, tumored mice were pretargeted with MORF-antibody, 48 h later were given an injection of ^{99m}Tc - or ^{111}In -cMORF, and finally were imaged repeatedly.

Results—The cMORF biodistribution in both normal and pretargeted tumored mice was influenced by its radiolabel. While excretion of both ^{99m}Tc -cMORF and ^{111}In -cMORF was rapid and mainly through the kidneys, about 2 % of ^{99m}Tc accumulated in the intestines compared to essentially no intestinal accumulation for ^{111}In at any time. Tumor accumulation was unchanged.

Conclusion—In applications of MORF/cMORF pretargeting intended to image organs deep within the abdomen such as the pancreas, radiolabeling with ^{111}In may be superior to ^{99m}Tc

Keywords

Pretargeting; Anticancer; Antibodies; Tumor; Radioimmunotargeting

Introduction

When compared to conventional nuclear imaging of tumor using radiolabeled antitumor antibodies, pretargeting, in which the radiolabel is administered on a small effector subsequent to the administration of the antitumor antibody, can improve tumor to normal tissue ratios [1-5] but only if the effector itself does not accumulate in normal organ. We are interested in applying a novel pretargeting approach using complementary phosphorodimaidate morpholino oligomers (i.e. MORF/cMORF) to image diseases of the pancreas. Thus far, conventional nuclear imaging of pancreatic cancer with radiolabeled antibodies has met with limited success due to poor pancreas/normal tissue ratios resulting from the accumulation of the radiolabeled antibodies in liver, spleen, intestines, kidneys and other organs of the abdomen [6,7]. A potential improvement may be possible by applying pretargeting to the imaging of this organ both for the early detection of cancer and for the imaging of normal pancreatic function in connection with noncancerous diseases such as diabetes. However, when radiolabeled with technetium-99m (^{99m}Tc) and administered to tumored and normal mice, the cMORF effector

developed in this laboratory accumulates in the kidneys and intestines. Since numerous reports confirm that radiolabeling with different radionuclides via different chelators can alter the pharmacokinetics of even large molecules such as antibodies [8-11], another imaging radionuclide, ^{111}In , was considered in this study as an alternative to $^{99\text{m}}\text{Tc}$. We now report on the reduced abdominal background level when the cMORF effector is labeled with ^{111}In in place of $^{99\text{m}}\text{Tc}$.

Material and Methods

As before, the base sequences of MORF and its complement (cMORF) were respectively 5'-TCTTCTACTTCACAACATA-linker-amine and 5'-TAGTTGTGAAGTAGAAGA-linker-amine (GeneTools, Philomath, OR). The DTPA was from Sigma (St Louis, MO) and the EDC (1-Ethyl-3(3-dimethylaminopropyl)carbodiimide hydrochloride) was from Pierce Company (Rockford, IL). The P-4 resin (Bio-Gel P-4 Gel, medium) was purchased from Bio-Rad Laboratories (Hercules, CA). The ^{99}Mo - $^{99\text{m}}\text{Tc}$ generator and the $^{111}\text{InCl}_3$ solution were both from Perkin Elmer Life Science Inc (Boston, MA). All other chemicals were reagent grade and used without purification.

The antiTAG-72 antibody CC49 was prepared for this investigation by Strategic Biosolutions (Ramona, CA) from the CC49 murine hybridoma cell line (a gift from Dr Schlom, Laboratory of Tumor Immunology and Biology, Center for Cancer Research, National Cancer Institute, NIH). Conjugation of MORF to the CC49 antibody was as reported previously in connection with other antibodies [12]. The Hydralink linker for the conjugation was from Solulink Biosciences (San Diego, CA).

Both the preparation of MAG_3 -cMORF and its use in the labeling with $^{99\text{m}}\text{Tc}$ were as previously described [13].

Preparation of DTPA-cMORF and radiolabeling with ^{111}In

To 333 μL of cMORF (1 mg) in 0.1 M, pH 5.0 MES was added 400 μL of a mixed solution (v/v = 1/5.4) of free DTPA (1 $\mu\text{g}/\mu\text{L}$) in deionized water and fresh EDC solution (4 $\mu\text{g}/\mu\text{L}$) in 0.1 M, pH 5.0 MES. After 2 h at room temperature, the mixture was purified on a 1 \times 50 cm P4 column (Bio-Rad, Hercules, CA) using 0.25 M, pH 5.2 NH_4AcO as eluent. The peak fractions were pooled. The molar ratios of DTPA/EDC/cMORF were 1/44/1. By adding tracer amount of ^{111}In before purification, the number of DTPA groups per cMORF (gpm) was calculated from the DTPA/cMORF molar ratio in the conjugation mixture and the fraction of radioactivity on the cMORF peak to be 0.17. For radiolabeling, at least 20 μL of the DTPA-cMORF stock solution was mixed with 1-5 μL $^{111}\text{InCl}_3$ solution. The labeled product was analyzed on a size-exclusion HPLC with a SuperdexTM 75 HR10/30 column (Amersham Pharmacia Biotech, Piscataway, NJ).

Animal studies

Two normal CD-1 mice (Charles River, Wilmington, MA) were anesthetized by IP injection of ketamine/xylazine (v/v = 90/10) and received an IV injection of either $^{99\text{m}}\text{Tc}$ -cMORF (5 μg , 2.7 mCi) or ^{111}In -cMORF (5 μg , 1.25 mCi), and were imaged over time on a NanoSPECT small animal camera with CT registration (Bioscan, Washington DC). Each of the acquisitions included 20 projections at 10 s per projection and required about 6-10 min. The total imaging time was a little more than one hour for each animal.

In groups of five, normal CD-1 mice received either $^{99\text{m}}\text{Tc}$ -cMORF (1 μg , 80 μCi) or ^{111}In -cMORF (1 μg , 10 μCi) and were sacrificed under anesthesia at 15 min. Samples of blood and organs were removed, weighted, and counted in a NaI(Tl) well counter (Cobra II automatic

gamma counter, Packard Instrument Company, CT) along with a standard of the injectate. Blood and muscle were assumed to constitute 7 % and 40 % of body weight respectively. The whole bladder including contents and the connected urethra and penis were excised and measured in a dose calibrator to estimate urine radioactivity.

Two NIH Swiss nude mice (Taconic Farms, Germantown, NY) were each implanted with LS174T tumor cells in the left thigh. At 13 day, when the tumors were 0.5-1.0 g, each mouse received 60 μg of MORF-CC49. Two days later, each mouse received 4.2 μg of cMORF labeled either with $^{99\text{m}}\text{Tc}$ (1.25 mCi) or ^{111}In (400 μCi). The dosages and timing were based on our previous experiences [14]. The $^{99\text{m}}\text{Tc}$ mouse was imaged at 3 and 10 h and the ^{111}In mouse was imaged at 3 h and 15 h. The mice were then sacrificed by exsanguination via heart puncture under halothane anesthesia. In addition to normal organs and tissues, the tumored thigh was excised and the skin and as much of the muscle and bone as possible were removed before counting. The radioactivity therein was attributed to the tumor since the radioactivity levels in bone and muscle were negligible. After the tumor thigh was counted, the tumor mass was dissected to isolate the residual bone and muscle so that their weights could be subtracted to provide the net tumor weight.

Results

Biodistributions of labeled cMORFs in normal mice

The labeling procedures for both $^{99\text{m}}\text{Tc}$ and ^{111}In provide a radiochemical purity of about 95% by size-exclusion HPLC. The fused anterior projections of the SPECT and CT reconstructed acquisition in normal mice receiving either with $^{99\text{m}}\text{Tc}$ -cMORF or ^{111}In -cMORF are shown in Fig 1 at two time points. Radioactivity in the bladder of both animals has been digitally removed by manually selecting the volume of interest. In the same manner ^{111}In urine contamination of the animal's coat was removed from the 68 min image. Whereas both radiolabels accumulated in the kidneys, $^{99\text{m}}\text{Tc}$ also accumulated predominately in the hepatobiliary tree including the gall bladder and small intestines. As expected for hepatobiliary accumulation, the $^{99\text{m}}\text{Tc}$ distribution moved over time.

The biodistribution results in normal mice via necropsy are shown in Table 1. The radioactivity levels for both radiolabels are almost identical in each organ except in liver, lung, gall bladder, and small intestines where the accumulation of ^{111}In is significantly lower (Student's t test, $p < 0.05$). For both $^{99\text{m}}\text{Tc}$ and ^{111}In , about 60 % of the administered radioactivity was in the bladder at 15 min.

Pharmacokinetics of labeled cMORFs in pretargeted mice

The distribution of radioactivity in two tumored nude mice pretargeted with MORF-CC49 antibody is shown in Fig 2 as posterior and right-lateral projections of the distributions at 3 and 10 h for $^{99\text{m}}\text{Tc}$ or at 3 and 15 h for ^{111}In . As expected from the results in normal mice, the accumulation of ^{111}In in the abdomen is minimal in comparison to that of $^{99\text{m}}\text{Tc}$. Unlike the projections of Fig. 1, higher accumulations of ^{111}In are apparent in the lung and liver compared to $^{99\text{m}}\text{Tc}$ in these pretargeted mice.

The radioactivity accumulations in tumor and kidneys in these two pretargeted mice have been estimated using IVS InvivoScope 1.35beta1 software (Bioscan). The average results of five independent observers are presented in Table 2 along with that obtained by necropsy. While the accumulations of $^{99\text{m}}\text{Tc}$ measured by image quantitation are in agreement with those by necropsy within 10%, this difference is about 40% in the case of ^{111}In .

Discussion

Although MORF/cMORF pretargeting has been used successfully for nuclear imaging of tumor in mice, the higher accumulations of radioactivity in the intestines following ^{99m}Tc -cMORF administration shown in Fig 1 and 2 may become problematic when imaging within the abdomen. As shown in Table 1, about 2 % of the administered ^{99m}Tc accumulates in the intestines in the first 15 min following IV administration. Furthermore if the accumulation is in the intestinal contents, as in this case, imaging may be made still more problematic by the motion of the contents over time. Fortunately, as shown by both imaging and necropsy, intestinal accumulation was about 4 fold lower in mice receiving the effector radiolabeled with ^{111}In .

As is evident in Fig 2, the accumulations in lung, liver and kidneys are higher in the pretargeted animals receiving ^{111}In -cMORF compared to ^{99m}Tc -cMORF. These higher accumulations were not seen in the mice that did not receive the pretargeting antibody (Fig 1) and therefore may be related to the MORF-antibody in circulation and in tissues at the time of the effector administration. While the lung accumulation of ^{111}In is seen only in the 3 h projections, the liver accumulations appear in both early and late projections. These higher liver accumulations may be due to the residualizing properties of ^{111}In compared to ^{99m}Tc [15,16].

In conclusion, the biodistribution of a cMORF effector in both normal and pretargeted tumored mice was influenced by its radiolabel. When labeled with ^{111}In via DTPA, accumulations in intestinal organs was minimal compared to the same effector radiolabeled with ^{99m}Tc via MAG_3 . Therefore in applications of MORF/cMORF pretargeting intended to image organs deep within the abdomen such as the pancreas, radiolabeling with ^{111}In may be superior to ^{99m}Tc .

Acknowledgment

The authors are grateful to Dr Jeffery Schlom (Laboratory of Tumor Immunology and Biology, Center for Cancer Research, NCI, NIH, Bethesda, MD) for providing the CC49 hybridoma. Financial support was from the National Institute of Health and Juvenile Diabetes Research Foundation International (CA94994, CA107360, and JDRF 37-2009-7).

References

1. Karacay H, Brard PY, Sharkey RM, Chang CH, Rossi EA, McBride WJ, Ragland DR, Horak ID, Goldenberg DM. Therapeutic advantage of pretargeted radioimmunotherapy using a recombinant bispecific antibody in a human colon cancer xenograft. *Clin Cancer Res* 2005;11:7879–7885. [PubMed: 16278412]
2. Sharkey RM, Cardillo TM, Rossi EA, Chang CH, Karacay H, McBride WJ, Hansen HJ, Horak ID, Goldenberg DM. Signal amplification in molecular imaging by pretargeting a multivalent, bispecific antibody. *Nat Med* 2005;11:1250–1255. [PubMed: 16258537]
3. Pagel JM, Hedin N, Subbiah K, Meyer D, Mallet R, Axworthy D, Theodore LJ, Wilbur DS, Matthews DC, Press OW. Comparison of anti-CD20 and anti-CD45 antibodies for conventional and pretargeted radioimmunotherapy of B-cell lymphomas. *Blood* 2003;101:2340–2348. [PubMed: 12446461]
4. Subbiah K, Hamlin DK, Pagel JM, Wilbur DS, Meyer DL, Axworthy DB, Mallett RW, Theodore LJ, Stayton PS, Press OW. Comparison of immunoscintigraphy, efficacy, and toxicity of conventional and pretargeted radioimmunotherapy in CD20-expressing human lymphoma xenografts. *J Nucl Med* 2003;44:437–445. [PubMed: 12621012]
5. Magnani P, Paganelli G, Modorati G, Zito F, Songini C, Sudati F, Koch P, Maecke HR, Brancato R, Siccari AG, Fazio F. Quantitative comparison of direct antibody labeling and tumor pretargeting in uveal melanoma. *J Nucl Med* 1996;37:967–971. [PubMed: 8683323]
6. Smith, Robert A.; Cokkinides, Vilma; Eyre, Harmon J. American Cancer Society Guidelines for the Early Detection of Cancer, 2006. *CA Cancer J Clin* 2006;56:11–25. [PubMed: 16449183]

7. Buchsbaum DJ. Experimental approaches to increase radiolabeled antibody localization in tumors. *Cancer Res* 1995;55:5729s–5732s. [PubMed: 7493336]
8. Hiltunen JV. Search for new and improved radiolabeling methods for monoclonal antibodies. A review of different methods. *Acta Oncol* 1993;32:831–839. [PubMed: 8305233]
9. Quadri SM, Vriesendorp HM. Effects of linker chemistry on the pharmacokinetics of radioimmunoconjugates. *Q J Nucl Med* 1998;42:250–261. [PubMed: 9973840]
10. Quadri SM, Vriesendorp HM, Leichner PK, Williams JR. Evaluation of indium-111- and yttrium-90-labeled linker-immunoconjugates in nude mice and dogs. *J Nucl Med* 1993;34:938–945. [PubMed: 8509861]
11. Liu G, Dou S, Pretorius PH, Liu X, Rusckowski M, Hnatowich DJ. Pretargeting CWR22 prostate tumor in mice with MORF-B72.3 antibody and radiolabeled cMORF. *Eur J Nucl Med Mol Imaging* 2008;35:272–280. [PubMed: 17909792]
12. Liu G, Dou S, Mardirossian G, He J, Zhang S, Liu X, Rusckowski M, Hnatowich DJ. Successful radiotherapy of tumor in pretargeted mice by ^{188}Re radiolabeled phosphorodiamidate morpholino oligomer, a synthetic DNA analog. *Clin Can Res* 2006;12:4958–1964.
13. Liu G, Dou S, He J, Yin D, Gupta S, Zhang S, Wang Y, Rusckowski M, Hnatowich DJ. Radiolabeling of MAG₃-morpholino oligomers with ^{188}Re at high labeling efficiency and specific radioactivity for tumor pretargeting. *Appl Radiat Isot* 2006b;64:971–978. [PubMed: 16730997]
14. Liu G, Dou S, He J, Liu X, Rusckowski M, Hnatowich DJ. Predicting the biodistribution of radiolabeled cMORF effector in MORF-pretargeted mice. *Eur J Nucl Med Mol Imaging* 2007;34:237–246. [PubMed: 17021815]
15. Duncan JR, Behr TM, DeNardo SJ. Intracellular fate of radiometals. *J Nucl Med* 1997;38:829. [PubMed: 9170459]
16. Duncan JR, Stephenson MT, Wu HP, Anderson CJ. Indium-111-diethylenetriaminepentaacetic acid-octreotide is delivered in vivo to pancreatic, tumor cell, renal, hepatocyte lysosomes. *Cancer Res* 1997;57:659–671. [PubMed: 9044843]

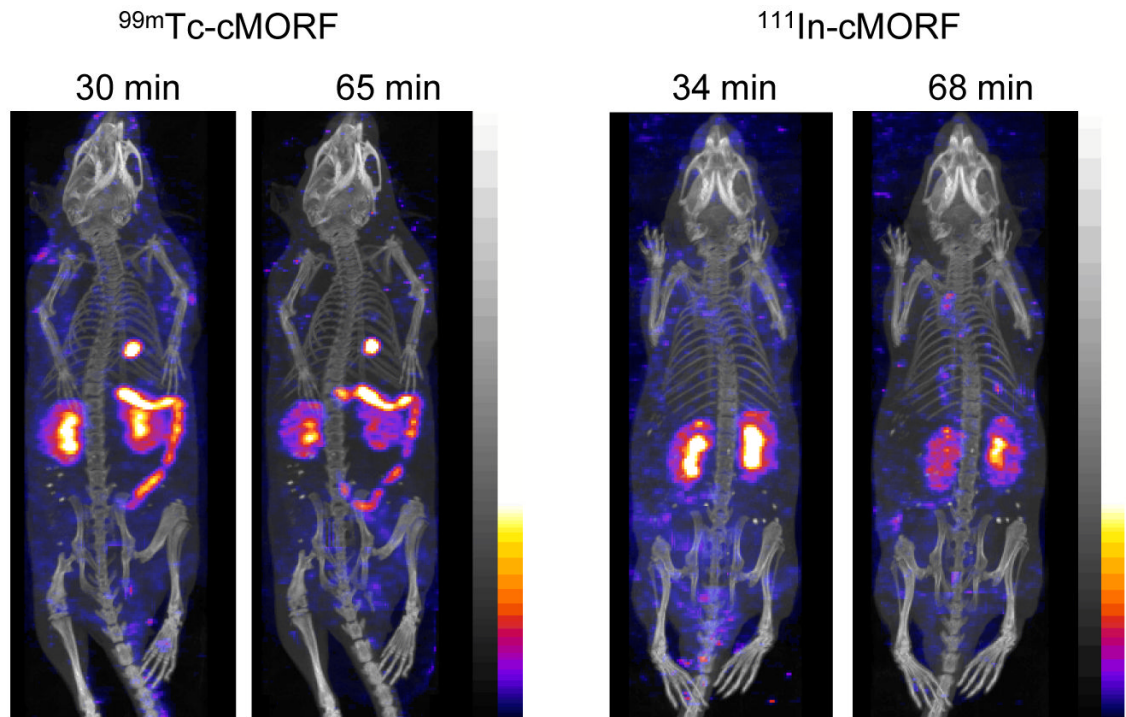


Fig 1. Anterior projections of the SPECT/CT fused acquisitions obtained at two time points in normal mice receiving either ^{99m}Tc -cMORF (left panel) or ^{111}In -cMORF (right panel). Bladder ^{99m}Tc and ^{111}In radioactivity were digitally removed in all projections as was the ^{111}In contamination on the animal's coat in the 68 min ^{111}In projection.

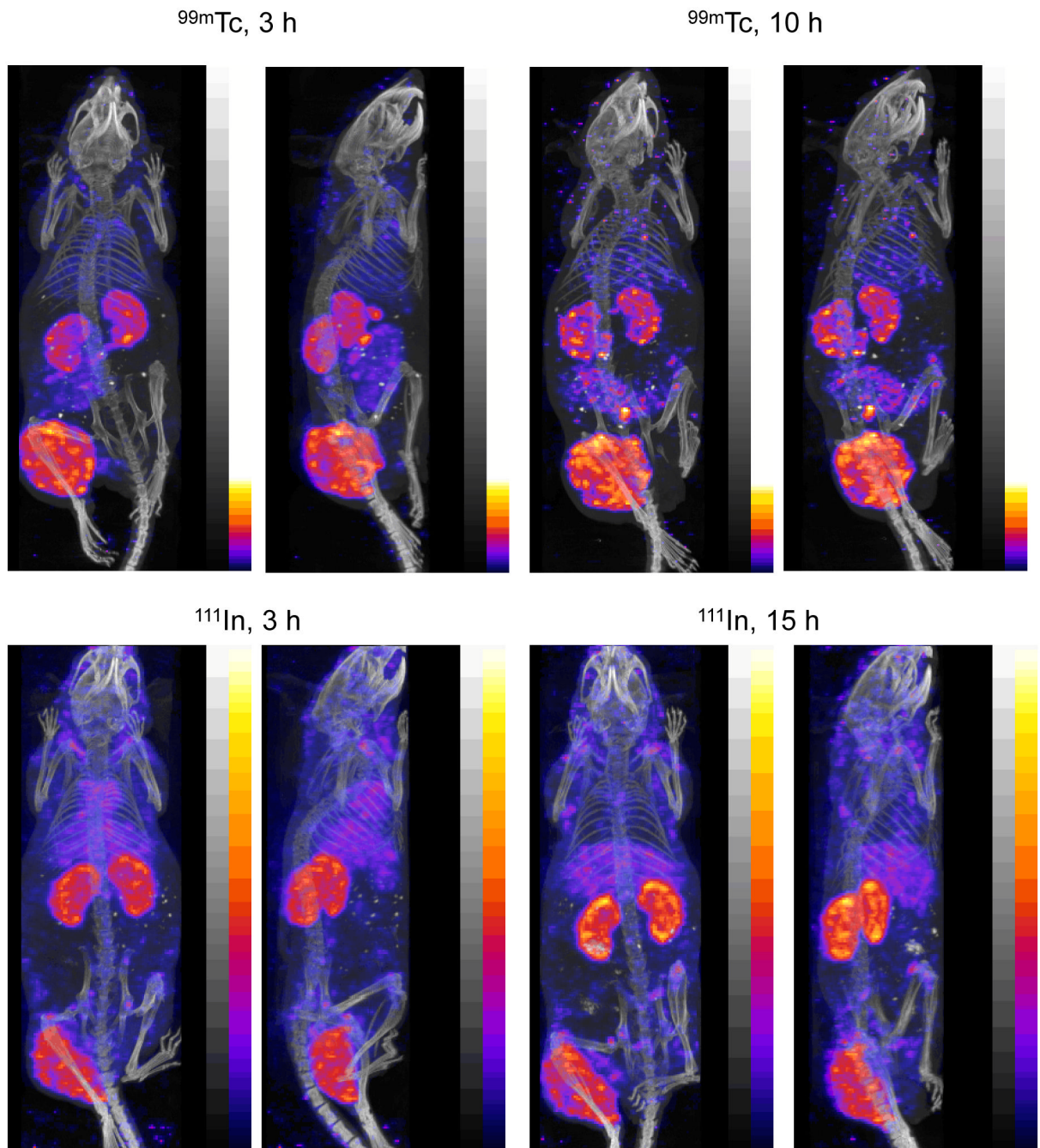


Fig 2. The posterior and right lateral projections of fused SPECT/CT acquisitions at two time points in tumored mice pretargeted with MORF-CC49 and injected with ^{99m}Tc -cMORF (top panels) or ^{111}In -cMORF (bottom panels). Bladder ^{99m}Tc and ^{111}In radioactivity have been digitally removed in all projections.

Biodistributions by necropsy in normal CD-1 mice receiving either $^{99m}\text{Tc-cMORF}$ or $^{111}\text{In-cMORF}$ 15 min earlier ($N = 5$). P values (Student's t test) for the differences between injection are also presented with those statistically significant ($p < 0.05$) italicized and underlined

Table 1

Organ	$^{111}\text{In-cMORF}$		$^{99m}\text{Tc-cMORF}$		P value
	Average	SD	Average	SD	
(a) %ID/g					
Liver	0.39	0.06	0.56	0.04	<u>0.00</u>
Heart	0.60	0.09	0.64	0.10	0.28
Kidney	10.13	2.72	9.80	4.35	0.45
Lung	1.14	0.14	1.60	0.33	<u>0.01</u>
Spleen	0.40	0.04	0.40	0.05	0.40
Pancreas	0.52	0.08	0.61	0.10	0.08
Muscle	0.80	0.43	0.57	0.12	0.14
Salivary gland	0.74	0.17	0.77	0.12	0.37
Blood	1.93	0.25	1.90	0.28	0.44
(b) %ID/organ					
Stomach	0.24	0.08	0.30	0.08	0.13
Small Intestine	0.79	0.18	2.69	0.26	<u>0.00</u>
Large intestine	0.31	0.03	0.33	0.07	0.29
Gall bladder	0.00	0.00	0.04	0.04	<u>0.03</u>

A comparison of tumor and kidney accumulations ($\mu\text{Ci}/\text{organ}$) at the time of necropsy for both $^{99\text{m}}\text{Tc}$ and ^{111}In by imaging at two time points with one standard deviation and by necropsy

Table 2

Organ	$^{99\text{m}}\text{Tc}$, 3 h		$^{99\text{m}}\text{Tc}$, 10 h		^{111}In , 3 h		^{111}In , 15 h	
	By imaging	By necropsy	By imaging	By necropsy	By imaging	By necropsy	By imaging	By necropsy
Tumor	19.6 ± 0.8	17.3	18.6 ± 0.4	17.3	17.2 ± 1.20	18.0 \pm 0.9	18.0 ± 0.9	10.4
Left kidney	3.9 ± 0.2	-----	3.1 ± 0.1	-----	8.9 ± 0.4	9.1 ± 0.2	9.1 ± 0.2	-----
Right kidney	4.6 ± 0.4	-----	3.3 ± 0.2	-----	9.1 ± 0.5	8.7 ± 0.7	8.7 ± 0.7	-----
Total kidneys	8.5 ± 0.3	6.8	6.4 ± 0.2	6.8	18.0 ± 0.8	17.8 ± 0.7	17.8 ± 0.7	11.2